University Library

MINERVA ACCESS

A gateway to Melbourne's research publications

Minerva Access is the Institutional Repository of The University of Melbourne

Author/s:
Farrell, MJ;Trevaks, D;McAllen, RM

Title:
Preoptic activation and connectivity during thermal sweating in humans

Date:
2014-09-30

Citation:
Farrell, M. J., Trevaks, D. & McAllen, R. M. (2014). Preoptic activation and connectivity during thermal sweating in humans. Temperature, 1 (2), pp.135-141. https://doi.org/10.4161/temp.29667.

Persistent Link:
https://hdl.handle.net/11343/260152

License:
CC BY-NC

RESEARCH PAPER

Temperature 1:2, 135–141; July/August/September 2014; © 2014 Landes Bioscience

Preoptic activation and connectivity during thermal sweating in humans

Michael J Farrell*, David Trevaks, and Robin M McAllen

The Florey Institute of Neuroscience and Mental Health; University Of Melbourne; Parkville, VIC Australia

Keywords: brain, fMRI, functional connectivity, preoptic area, sweating

Animal studies have identified the preoptic area as the key thermoregulatory region of the brain but no comparable information exists in humans. We used fMRI to study the preoptic area of human volunteers. Subjects lay in a 3T MRI scanner and were subjected to whole body heating by a water-perfused suit, to a level that resulted in a low rate of discrete sweating events (measured by finger skin resistance). Control scans were taken under thermoneutral conditions in another group. A discrete cluster of voxels in the preoptic area showed activity that was significantly correlated with thermal sweating events. We then used this cluster as a seed to investigate whether other brain areas had activity correlated with its signal, and whether that correlation depended on thermal state. Several brain regions including the dorsal cingulate cortex, anterior insula and midbrain showed ongoing activity that was correlated with that of the preoptic seed more strongly during heating than during thermoneutrality. These data provide the first imaging evidence for a thermoregulatory role of the human preoptic area. They further suggest that during thermal stress, the preoptic area communicates to several other brain regions with known relevance to the control of autonomic effectors.

Introduction

Converging lines of evidence strongly support the conclusion that the preoptic area (POA) is a critical brain region for thermoregulatory control.[1] However, studies implicating the POA as a thermoregulatory region have been confined to animal research. It is reasonable to assume that the analogous region in the human is also likely to play a role in thermoregulation, although this is yet to be demonstrated. The objective of this study was to measure signals from the POA during neutral and heating conditions to establish if the region shows thermoregulatory responses in humans.

The brain control of thermoregulation and associated sensations has been investigated in humans using positron emission tomography (PET) and functional magnetic resonance imaging (fMRI). These studies have identified brainstem nuclei with responses associated with heating-related sweating[2] and cooling-related vasoconstriction,[3] as well as hemispheric regions that activate during whole-body heating and cooling,[4] including regions that activate in association with temperature sensations.[5-7] Activation in the POA was not reported in these studies, and this absence is probably a consequence of methodological issues. The POA is a relatively small structure in the context of human functional brain imaging techniques and the studies of thermoregulation reported thus far did not include optimal methods for the identification of activation in a small region. In some studies the field of view did not include the POA[2,3] and in others the spatial resolution of the imaging modality was insufficient to identify activity in small regions.[4,5] In another study the experimental design incorporated slowly changing conditions that are not ideal for the execution of fMRI, thus decreasing the likelihood of finding signal changes from a relatively small structure.[6]

As this juncture, functional brain imaging studies have not implicated the POA as a thermoregulatory region in humans. Attempting to address this shortfall is appealing for several reasons. First, it extends our understanding of thermoregulation by the brain to a new species—one in which we have a particular interest. Second, it is straightforward to investigate conscious subjects, without preparatory surgery. Third, the involvement of other brain regions in thermoregulatory processes can be probed at the same time.

Sweating is an important heat loss mechanism that is highly developed in humans. We have previously used blood oxygen level dependent (BOLD) signals to reveal sweating-related activation in the dorsal midbrain and the rostral lateral medulla. The latter location corresponds to an area shown to drive sweating in cats,[8] and probably gives rise to the final descending pathway to the spinal sympathetic sudomotor neurons. Activation of that cell group was common to both thermal and mental sweating.[2] Above the brain stem it is likely that the regions driving thermal and psychogenic sweating diverge. Several studies have identified forebrain sites that are activated during psychogenic sweating,[9,10] but no clear source of thermogenic sweating has yet been identified. The present study used a region of interest analysis to test

*Correspondence to: Michael J Farrell; Email: michael.farrell@florey.edu.au
Submitted: 05/31/2014; Revised: 06/19/2014; Accepted: 06/19/2014; Published Online: 07/01/2014
http://dx.doi.org/10.4161/temp.29667

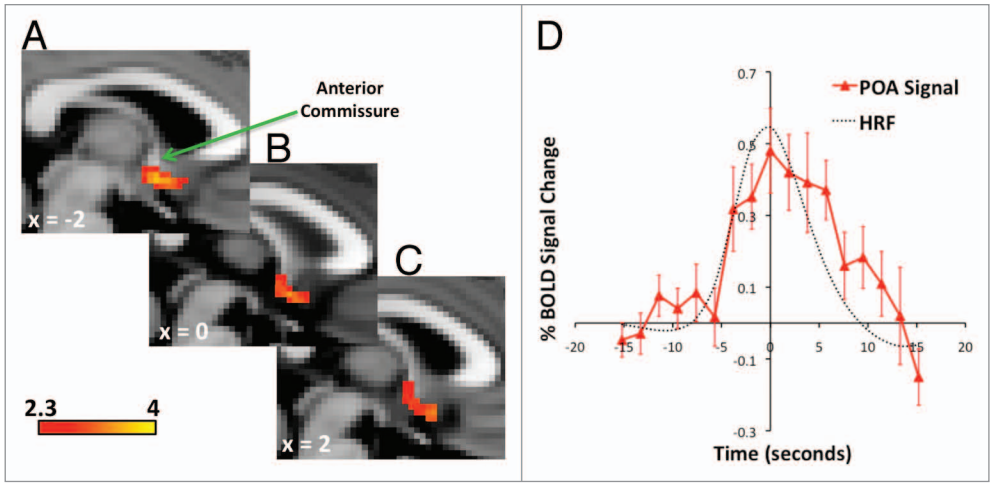


Figure 1. (**A**) A cluster of sweating activation occurred in a region encompassing the POA. The peak of the cluster was 2mm into the left hemisphere immediately inferior to the anterior margin of the anterior commissure. (**B**) The POA cluster of sweating activation extended across the midline, and (**C**) into the right hemisphere. (**D**) The signals were extracted from the POA cluster and divided into 32.2 s periods centered around peaks of sweating events. The sweating divisions were averaged for each participant and then a grand mean was calculated for the sample. The grand mean time course shows the increases predicted by a similar average of hemodynamic response functions (HRF). Activation $P_{corrected} < 0.05$. Positions of slices labeled according to convention where +ve x = distance in mm to right of midline, x = 0 is at midline, and –ve x = distance in mm to left of midline.

the hypothesis that the preoptic area is involved in thermogenic sweating.

Results

Skin temperature

Heating was associated with increased skin temperature compared with the neutral state (neutral 33.3 ± 1.5, heating 36.4 ± 1.3, $t^{18} = 5.0$, $P < 0.001$).

Sweating activation

A midline cluster of sweating activation (cluster corrected, $P_{corrected} < 0.05$) was identified inferior to the anterior commissure (**Fig. 1A–C**). The peak of the POA cluster was at x = –2 (2mm to the left of midline), y = 2 (2mm anterior of the posterior edge of the anterior commissure), z = –10 (10 mm inferior to the superior edge of the anterior commissure) and had a value of z = 3.21. Sweating activation at a cluster corrected threshold also occurred at many other sites in the brain, but these were beyond the region of interest and are not reported.

Signals extracted from the cluster of sweating activation showed significant temporal changes during repeated sweating events ($F[16,160] = 3.6$, $P < 0.001$). Post hoc pair-wise comparisons revealed differences between baseline and time points before the sweating peak (–3.8sec $t^{10} = 3.0$ $P < 0.01$, –1.9sec $t^{10} = 3.8$ $P < 0.005$), at the peak ($t^{10} = 3.7$ $P < 0.005$) and after the peak (1.9sec $t^{10} = 3.7$ $P < 0.005$, 3.8sec $t^{10} = 3.1$ $P < 0.01$, 5.7sec $t^{10} = 4.8$ $P < 0.001$) (**Fig. 1D**).

POA functional connectivity

Levels of inter-regional correlation (functional connectivity) with the POA were significantly increased during heating compared with neutral in a widely distributed network of brain regions ($P_{corrected} < 0.05$). Regions in the network included limbic cortices (cingulate cortex), paralimbic cortices (insula), prefrontal regions (middle frontal gyrus, inferior frontal gyrus) parietal cortices (inferior parietal lobule, precuneus), thalamus, putamen, midbrain, pons, and cerebellum (**Fig. 2**; **Table 1**).

Discussion

To the best of our knowledge this is the first neuroimaging study to implicate the human POA in thermoregulation. The study identifies the POA as a likely source of the thermal drive to sweat in humans. The functional connectivity from the POA during body heating further suggests forebrain regions that are likely to be involved in heat defense.

Unlike previous reports of thermoregulatory-related regional brain responses in humans, this study clearly demonstrated activation in the POA. It is very likely that aspects of the methodology facilitated the demonstration of POA activation. Most notably, the focus on thermal sweating meant that events of interest occurred with durations and frequencies that were least likely to be conflated with other attributes of the BOLD signal such as lower frequency scanner-related drift and higher frequency physiological noise.[11] The approach led to robust levels of sweating-related responses in the POA. The cluster of activation had a peak and spatial distribution that was consistent with the anatomical location of the POA, immediately inferior to the anterior commissure. In fact, the cluster of voxels with sweating-related activation showed signals strong enough to pass very conservative threshold criteria and the sweating-related BOLD signal changes closely matched the expected response.

The POA in animals has been shown to contain temperature sensitive neurons and, when heated, to activate multiple heat loss responses including sweating. The current view is that distinct thermosensitive POA neurones drive each thermoregulatory response.[12,13] Although the current experimental paradigm

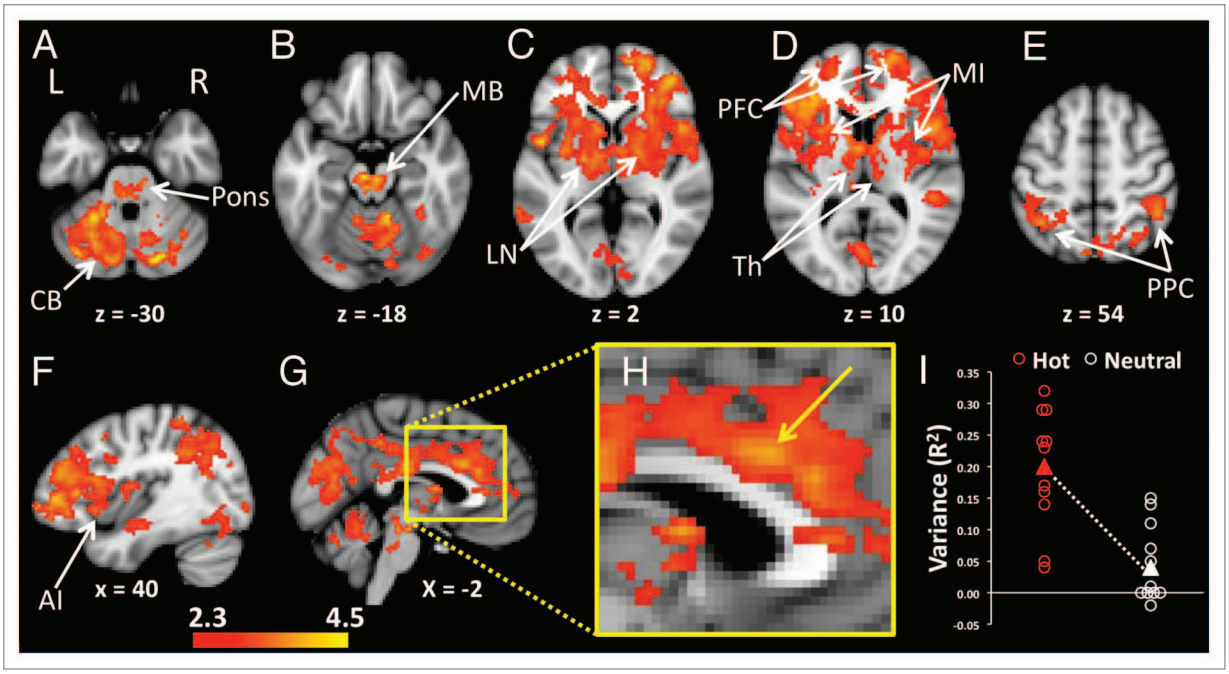


Figure 2. Increased levels of functional connectivity with the POA during heating compared with the neutral condition were seen in widely distributed regions of the brain. (**A**) The pons and bilateral regions of the cerebellum (CB) showed heating-related increases of POA connectivity. (**B**) Enhanced POA connectivity was also apparent in midbrain (MB), (**C**) lentiform nuclei (LN), (**D**) bilateral thalamus (Th), mid insula (MI), prefrontal cortices (PFC), (**E**) and bilateral posterior parietal cortices (PPC). (**F**) The anterior insula (AI) in the right hemisphere showed heating-related increases in connectivity with the POA. (**G**) Mesial regions including the midcingulate cortex, posterior cingulate cortex and precuneus had increased POA connectivity during heating. (**H**) An enlarged image of the mesial surface of the brain shows the location of increased POA connectivity in the midcingulate cortex The arrow indicates the voxel with the highest statistic (z = 3.73) in the slice at x = –2, y = 18, z = 28. (**I**) Signals from the midcingulate region, shown in **H**, were extracted and correlated with the corresponding POA seeds in order to visualize the distribution of variances between the two groups of participants. Activations $P_{corrected} < 0.05$. Background image is MNI template brain and axial slices are oriented to show right side of brain on right side of image. Positions of slices labeled according to convention where +ve z = distance in mm superior to anterior commissure, -ve z = distance in mm inferior to anterior commissure, +ve x = distance in mm to right of midline, -ve x = distance in mm to left of the midline. Axial images (**A–E**) are displayed with the right side of the brain on the right side of the image.

identified sweating-related activity in the POA, it is likely that multiple heat loss neuronal circuits are located within this territory. Indeed, these multiple circuits were likely to have contributed to the distribution of regions showing heating-related increases of POA functional connectivity. While the POA seed was defined as sweat activated voxels, and sweating-related change was consequently a significant component of the signal, other heating-related processes would contribute to signal variance, which in turn could be correlated with functionally connected brain regions.

The network of regions showing heating-related POA functional connectivity was widely distributed throughout the brain. Regions in the ventral and dorsal midbrain were among the clusters functionally connected to the POA. The loci of the clusters in the midbrain are similar to regions with heating-related sweating activation reported in a study using images optimized for the brainstem,[2] thus providing converging evidence for a sweating control circuit in humans incorporating the POA and midbrain. Another brainstem region that has previously shown thermal sweating activation, the rostral lateral medulla,[2] was not among the correlates of the POA seed. However, the small size of the rostral lateral medulla militated against significant connectivity in this region at a conservative threshold. Future studies involving images optimised for the brainstem and hypothalamus will be required to more definitively test the level of correlated signal between the POA and rostral lateral medulla.

The extensive regions in the hemispheres showing heating-related connectivity with the POA are likely to represent complimentary heat defense processes including, but not restricted to sweating control. These processes could relate to functions putatively contingent on POA inputs such as temperature sensation, motor responses, autonomic responses and arousal, although the associative nature of the analysis does not permit any discrimination between regions on functional grounds. Nevertheless, it is salient to note the presence of symmetrical clusters of POA connectivity in the anterior midcingulate (dorsal) cortex and a cluster in the right anterior insula. A growing body of evidence from human neuroimaging and lesion studies have highlighted the anterior midcingulate cortex as a central region in the behaviorally integrated control of autonomic responses, including sweating,[14] whereas the insula cortex has emerged as a major site involved in the representation of bodily states.[15] Additionally, the cluster with a locus in the right anterior midcingulate cortex extended in the posterior midcingluate cortex to incorporate a region previously implicated in the representation of thermal discomfort.[5] It is possible that functional connectivity between

Table 1. POA functional connectivity, heating greater than neutral

Region	BA	Side	Coordinates			Z score
			x	y	z	
Middle Frontal Gyrus	9	R	34	38	34	7.68
	9	L	–42	24	28	3.55
	46	R	46	28	24	3.42
	46	L	–34	44	26	3.77
	10	R	42	46	4	4.00
	10	R	26	56	–2	4.23
	10	L	–22	48	–4	3.40
Inferior Frontal Gyrus	45	R	52	16	12	3.75
	45	L	–52	30	10	3.80
Midcingulate Cortex	24	R	2	28	22	3.57
	24	L	–4	16	28	3.71
Posterior Cingulate Cortex	23	R	6	–28	36	4.19
	23	L	–4	–24	28	3.83
Inferior Parietal Lobule	40	R	46	–46	54	3.46
	40	L	–36	–52	56	4.08
	40	R	50	–46	42	3.17
	40	L	–48	–56	40	3.45
Parietal Operculum (SII)		R	60	–22	24	3.42
Precuneus	7	R	8	–66	36	3.15
	7	L	–8	–70	36	3.15
Insula	13	R	46	12	10	3.67
	13	L	–30	10	10	3.44
	13	R	44	18	–6	3.27
	13	L	–34	–2	6	3.32
Medial Dorsal Thalamus		R	10	–20	12	3.53
		L	–6	–12	12	3.26
Putamen		R	20	6	0	3.21
		L	–16	10	0	3.11
Globus Pallidus		R	18	–4	2	3.38
		L	–20	–8	2	3.59
Caudate		L	–10	12	4	3.30
Dorsal Midbrain		R	12	–24	–10	3.31
		L	–8	–26	–10	3.12
Ventral Midbrain			–4	–20	–18	4.27
Pons		R	4	–34	–32	3.65
XX		L	–6	–36	–32	3.85
Cerebellum						
Declive		R	22	–76	–28	5.26
Folium		L	–38	–74	–30	3.87
Pyramis		R	18	–56	–48	4.71
Pyramis		L	–16	–62	–46	4.94

BA, Brodmann area; R, right; L, left; coordinates, position of peak voxel of activated cluster in space of MNI standard brain; x, distance in mm right (+ve) or left (-ve) from midline; y, distance in mm anterior (+ve) or posterior (–ve) from the anterior commissure; z, distance in mm superior (+ve) or inferior (–ve) from the anterior commissure; Z score, standardized statistic of activation level of peak voxel of activated cluster.

cortical regions and the POA could be related to interactions that orchestrate heat defenses.

Summary

This study has effectively added humans to the list of species showing activity in the POA associated with heat defense. Sweating activation is clearly localized to the POA in humans, and signals from the region show levels of functional connectivity with distributed brain regions that are heating-related. The successful demonstration of sweating activation in the POA will provide impetus and a sound basis for future studies of thermoregulatory processes in humans.

Materials and Methods

Participants

This study was approved by the Melbourne Health Human Research Ethics Committee (approval 2008.147). All volunteers recruited for the study provided informed consent to participate according to approved procedures. A previous report of data obtained from this sample has been reported.[2] Two groups of 11 people were involved. Both groups consisted on ten men and one woman and were aged 34.4 (± 10.2) and 35.3 (± 11.8) years. Four males were included in both groups. The data acquired from the participants and reported in this manuscript has not been published previously.

Thermal stimulation

One group of participants underwent whole body heating. Participants in the heating group wore a body suit (Med-Eng BCS4 Body Cooling System, Allen Vanguard) incorporating 4mm plastic tubing that was connected to a water reservoir and pump as previously described.[2] The water in the reservoir was heated to between 40 and 50 °C and then circulated through the network of tubing in the suit. Heating was maintained to achieve regular sweating, during which images of the brain were acquired. Brain images were also acquired from the second group of participants who were not heated. Both groups were instructed to lie still throughout image acquisition, and neither group performed any active tasks during scanning.

Measurement of Electrodermal Responses and Skin Temperature

Electrodermal responses were recorded from all participants using two Ag-AgCl electrodes (TSD203 electrodes, Biopac Systems) connected to the right index and middle fingers as previously described.[2] Signals from the electrodes were digitized at 1khz and recorded to computer (Spike2, Cambridge Electronic Design). The onset and offset of electrode recordings were triggered by signals from the scanner console so that the timing of electrodermal responses could be matched to the timing of image acquisitions. Responses were recorded as AC signals (0.5Hz high pass filter) to identify discrete electrodermal events independently of any shift in mean signal level. Type T (copper – constantan) thermocouples were attached to three different sites on participants' trunks and an averaged signal was recorded via an electronic thermometer (Physitemp TH-5, Physitemp Instruments). The respiration signal was not successfully recorded in the majority of participants and consequently has not been reported here.

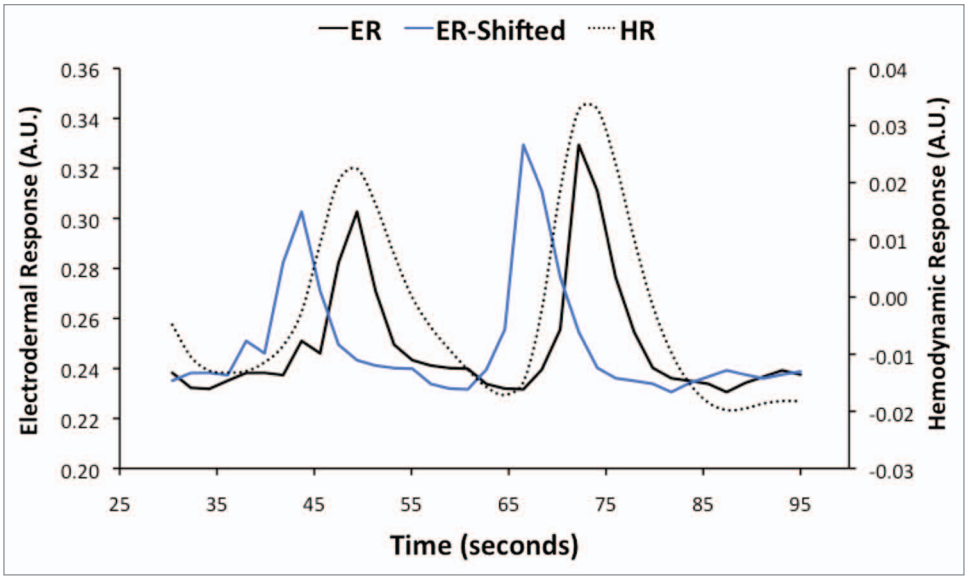


Figure 3. Electrodermal responses (ER) recorded during scanning were used in analyses of functional brain images to identify sweating activation. A representative example of ER early in a scanning run from a single participant is reproduced here. Brain activity associated with sweating occurs more than 5 s before sweating events. The ER was shifted backward in time by 5.7 s (ER-Shifted) to take account of the lag between neural activity and the observed occurrence of a sweating event. The fMRI signal is sensitive to hemodynamic responses driven by neural activity. The onsets and peaks of hemodynamic responses are delayed after neural activity by 2 to 6 s. The ER-Shifted was adjusted in accordance with the temporal properties of hemodynamics to produce a hemodynamic response function (HRF) that was used in the functional brain imaging analysis.

Image acquisition

A Siemens 3Tesla magnetic resonance imaging scanner (Trio system) with a 32-channel head coil at the Murdoch Children's Research Institute was used to acquire brain images for the study. High resolution structural images of participants' brains were collected using a T1 weighted image acquisition (192 × 0.9mm sagittal slices, 256 × 256 matrix, in-slice resolution 0.8mm × 0.8mm, TR = 1900ms, TE = 2.59ms, flip angle = 9 degrees). Functional brain images sensitive to blood oxygen level-dependent (BOLD) contrast were acquired from both groups (TR = 1900ms, TE = 35ms, flip angle = 90°). The field of view of the functional images encompassed the brain hemispheres, cerebellum and brainstem (30 slices of 4mm thickness, in-slice resolution = 3.6 × 3.6mm). Each functional scanning run involved the acquisition of 250 sequential brain volumes during 7minutes and 55 s (1.9 s per brain volume).

Analysis

Pre-processing

All processing of functional images was performed with the Oxford Centre for Functional Magnetic Resonance Imaging of the Brain Software Library (FMRIB, Oxford, FSL version 4.1 http://www.fmrib.ox.ac.uk/fsl/)). Sequential functional brain images were co-registered with the image acquired at the mid time point of a scanning run to correct for any head movement during acquisition.[16] The motion corrected sequential images were high passed filtered to remove low frequency signal drift, and spatially smoothed with a 6mm Gaussian kernel. Transformation matrices were calculated to register functional brain images to the Montreal Neuroscience Institute (MNI) template brain (voxel dimensions 2 × 2 × 2mm^3)[17,18] using a two-stage process. The first step involved co-registration of participants' low-resolution functional brain images (middle image used for motion correction) to their high-resolution structural images. In the second step participants' high-resolution structural images were warped to the template brain. The matrices resulting from the two steps were multiplied so that outcomes of image analyses could be transformed from each participant's functional image space to the common template space. All registrations and transformations were performed with the FMRIB Linear Image Registration Tool (FLIRT).[16,19,20]

Statistical analysis

Two analyses of participants' functional images were performed: sweat activation analysis and POA functional connectivity analysis.

Sweat activation analysis

The objective of the sweat activation analysis was to determine if BOLD signals measured in the region of the POA showed changes that correlated with the occurrence of sweating events. Analyses were confined to the images acquired during heating.

Adjustments were made to the electrodermal measures to allow for correlation with the BOLD signals. First, electrodermal measures were down-sampled to provided one measure each 1.9 s corresponding with the time to acquire a single functional image of the brain (**Fig. 3**). Electroencephalography measures have previously established that brain signal changes precede sweating events by 5 to 5.5 s on average.[21] Thus, to more accurately represent the likely timing of sweat-related regional brain activity, the down-sampled electrodermal measures were shifted back in time by 5.7 s, which is equivalent to the time taken to acquire three functional images of the brain (3 × 1.9 = 5.7) (**Fig. 3**). These time-shifted electrodermal measures were then adjusted to represent the expected BOLD signal changes contingent on the

hemodynamic responses driven by neural processes contributing to sweating. The peaks of hemodynamic responses usually lag neural activity by 4 to 6 s.[22] Consequently, the peaks of sweating-related BOLD signal changes were expected to occur at similar times to the real-time electrodermal recordings (**Fig. 3**).

The time-shifted electrodermal measures adjusted for hemodynamics were used in general linear model analyses to predict variance in BOLD signals related to sweating during whole body heating. Analyses were performed with the FMRI Expert Analysis Tool (FEAT) incorporating FMRIB's Improved Linear Model (FILM).[23] Additional regressors were included in the analysis to take account of confounding sources of variance related to head movement (motion correction parameters) and non-neural noise (i.e., nonsense signals extracted from white matter, ventricles and sagittal sinus).[24] Analyses produced a parameter for each voxel in the functional brain image of a participant that represented the correlation between the sequential time series of BOLD signal changes in the voxel and the adjusted electrodermal measure after taking account of the confounds. Collectively, participant's three-dimensional images of voxels coded with parameter estimates constituted statistical parametric maps (SPM). SPM from each participant were warped to the template brain using the transformation matrices described earlier. Warped SPM were entered in an analysis to determine the average level of response across the group. The group SPM incorporated standardised statistics (z-scores) that were thresholded at $z > 2.3$ to show voxels with sweating-related signal changes. Further thresholding based on the spatial extent of contiguous voxels with values of $z > 2.3$ was performed according to standard procedures to show clusters of activation by making corrections for significance that acknowledge the multiple comparisons performed across the whole brain (cluster corrected – $P < 0.05$).[25] The whole brain cluster thresholded map was examined to identify activation in the region of the POA.

BOLD signals were extracted from an activated cluster incorporating the POA to visualize sweating related changes. A search was performed in the template brain space to locate a cluster or clusters in a space based on the anatomy of the POA. The search space was located within the midline sagittal slice and the adjacent slices in the left and right hemispheres, spanning 10 × 10mm in the space inferior to the anterior commissure. The most superior, posterior corner of the search space was located at the inferior, posterior margin of the anterior commissure (coordinate $x = 0$, $y = 0$, $z = -4$ in the MNI template brain). A region of interest (ROI) was subsequently defined as activated voxels within the search area. The ROI was transformed to the spaces of each participant's functional brain images using the inverses of the transformation matrices described earlier. The transformed ROI were used as masks to extract and average the signal intensities of constituent voxels for each time point from sequential, pre-processed images (i.e., motion corrected, high pass filtered, spatially smoothed). Sweating-related signal change was characterized according to the timing of sweating events extrapolated from the adjusted electrodermal measures. The timing of electrodermal peaks were used as mid points in time series including eight preceding and eight subsequent points ($17 \times 1.9 = 32.2$ s). Signals from ROI for time series corresponding to electrodermal peaks were averaged for each participant and expressed as the percentage difference from the mean of the first three time points in the series. The averaged percentage signal changes from each participant were used to calculate a grand mean response.

POA functional connectivity analysis

The objective of the functional connectivity analysis was to identify brain regions whose signal was more strongly correlated with that of the POA during heating, compared with neutral thermal conditions. Functional brain images from both groups were used to test for the effects of heating on the functional connectivity of the POA.

A seed based functional connectivity analysis was performed in which signals extracted from the POA were used as regressors in general linear models to find brain regions where signal changes across time correlated with the POA seed. The POA seed used in the analysis consisted of the signals from the ROI identified by the sweating activation analysis. The POA seeds were entered as independent variables in general linear models to predict variance in BOLD signals throughout the brain. The inputs into these analyses were pre-processed functional brain images (motion corrected, high pass filtered, spatially smoothed). Confounds added to the model included motion parameters and signals extracted from regions including the white matter, ventricles and sagittal sinus. SPM resulting from the analyses of participants' functional brain images were transformed to the MNI template space for group analysis. The group analysis tested for differences between heating and neutral conditions in the regional levels of correlation with the POA seed. The SPM resulting from the group analysis was thresholded to identify corrected clusters among voxels with $z > 2.3$.

Disclosure of Potential Conflicts of Interest

No potential conflicts of interest were disclosed.

Acknowledgments

We acknowledge the technical expertise provided by Michael Kean of the Children's Magnetic Resonance Imaging Centre, Melbourne, Australia. This work was supported by the National Health and Medical Research Council (project Grant 509089, and Principal Research Fellowship 566667 to R.M.) and by the Victorian government through the Operational Infrastructure Scheme. M.J.F. received support from the Robert J. Kleberg, Jr. and Helen C. Kleberg Foundation and the G. Harold and Leila Y. Mathers Charitable Foundation.

References

1. Nakamura K. Central circuitries for body temperature regulation and fever. Am J Physiol Regul Integr Comp Physiol 2011; 301:R1207-28; PMID:21900642; http://dx.doi.org/10.1152/ajpregu.00109.2011
2. Farrell MJ, Trevaks D, Taylor NA, McAllen RM. Brain stem representation of thermal and psychogenic sweating in humans. Am J Physiol Regul Integr Comp Physiol 2013; 304:R810-7; PMID:23535458; http://dx.doi.org/10.1152/ajpregu.00041.2013
3. McAllen RM, Farrell M, Johnson JM, Trevaks D, Cole L, McKinley MJ, Jackson G, Denton DA, Egan GF. Human medullary responses to cooling and rewarming the skin: a functional MRI study. Proc Natl Acad Sci U S A 2006; 103:809-13; PMID:16407125; http://dx.doi.org/10.1073/pnas.0509862103
4. Egan GF, Johnson J, Farrell M, McAllen R, Zamarripa F, McKinley MJ, Lancaster J, Denton D, Fox PT. Cortical, thalamic, and hypothalamic responses to cooling and warming the skin in awake humans: a positron-emission tomography study. Proc Natl Acad Sci U S A 2005; 102:5262-7; PMID:15793009; http://dx.doi.org/10.1073/pnas.0409753102
5. Farrell MJ, Johnson J, McAllen R, Zamarripa F, Denton D, Fox PT, Egan GF. Brain activation associated with ratings of the hedonic component of thermal sensation during whole-body warming and cooling. J Therm Biol 2011; 36:57-63; http://dx.doi.org/10.1016/j.jtherbio.2010.11.003
6. Kanosue K, Sadato N, Okada T, Yoda T, Nakai S, Yoshida K, Hosono T, Nagashima K, Yagishita T, Inoue O, et al. Brain activation during whole body cooling in humans studied with functional magnetic resonance imaging. Neurosci Lett 2002; 329:157-60; PMID:12165401; http://dx.doi.org/10.1016/S0304-3940(02)00621-3
7. Sung EJ, Yoo SS, Yoon HW, Oh SS, Han Y, Park HW. Brain activation related to affective dimension during thermal stimulation in humans: a functional magnetic resonance imaging study. Int J Neurosci 2007; 117:1011-27; PMID:17613111; http://dx.doi.org/10.1080/00207450600934432
8. Shafton AD, McAllen RM. Location of cat brain stem neurons that drive sweating. Am J Physiol Regul Integr Comp Physiol 2013; 304:R804-9; PMID:23467325; http://dx.doi.org/10.1152/ajpregu.00040.2013
9. Critchley HD, Corfield DR, Chandler MP, Mathias CJ, Dolan RJ. Cerebral correlates of autonomic cardiovascular arousal: a functional neuroimaging investigation in humans. J Physiol 2000; 523:259-70; PMID:10673560; http://dx.doi.org/10.1111/j.1469-7793.2000.t01-1-00259.x
10. Critchley HD, Elliott R, Mathias CJ, Dolan RJ. Neural activity relating to generation and representation of galvanic skin conductance responses: a functional magnetic resonance imaging study. J Neurosci 2000; 20:3033-40; PMID:10751455
11. Parrish TB, Gitelman DR, LaBar KS, Mesulam MM. Impact of signal-to-noise on functional MRI. Magn Reson Med 2000; 44:925-32; PMID:11108630; http://dx.doi.org/10.1002/1522-2594(200012)44:6<925::AID-MRM14>3.0.CO;2-M
12. McAllen RM, Tanaka M, Ootsuka Y, McKinley MJ. Multiple thermoregulatory effectors with independent central controls. Eur J Appl Physiol 2010; 109:27-33; PMID:19949811; http://dx.doi.org/10.1007/s00421-009-1295-z
13. Nagashima K, Nakai S, Tanaka M, Kanosue K. Neuronal circuitries involved in thermoregulation. Auton Neurosci 2000; 85:18-25; PMID:11189023; http://dx.doi.org/10.1016/S1566-0702(00)00216-2
14. Critchley HD, Nagai Y, Gray MA, Mathias CJ. Dissecting axes of autonomic control in humans: Insights from neuroimaging. Auton Neurosci 2011; 161:34-42; PMID:20926356; http://dx.doi.org/10.1016/j.autneu.2010.09.005
15. Craig AD. Significance of the insula for the evolution of human awareness of feelings from the body. Ann N Y Acad Sci 2011; 1225:72-82; PMID:21534994; http://dx.doi.org/10.1111/j.1749-6632.2011.05990.x
16. Jenkinson M, Bannister P, Brady M, Smith S. Improved optimization for the robust and accurate linear registration and motion correction of brain images. Neuroimage 2002; 17:825-41; PMID:12377157; http://dx.doi.org/10.1006/nimg.2002.1132
17. Collins DL, Neelin P, Peters TM, Evans AC. Automatic 3D intersubject registration of MR volumetric data in standardized Talairach space. J Comput Assist Tomogr 1994; 18:192-205; PMID:8126267; http://dx.doi.org/10.1097/00004728-199403000-00005
18. Evans AC, Collins DL, Mills SR, Brown ED, Kelly RL, Peters TM. 3D statistical neuroanatomical models from 305 MRI volumes. Proceedings of IEEE-Nuclear Science Symposium and Medical Imaging Conference. 1993:1813-7.
19. Greve DN, Fischl B. Accurate and robust brain image alignment using boundary-based registration. Neuroimage 2009; 48:63-72; PMID:19573611; http://dx.doi.org/10.1016/j.neuroimage.2009.06.060
20. Jenkinson M, Smith S. A global optimisation method for robust affine registration of brain images. Med Image Anal 2001; 5:143-56; PMID:11516708; http://dx.doi.org/10.1016/S1361-8415(01)00036-6
21. Homma S, Nakajima Y, Toma S, Ito T, Shibata T. Intracerebral source localization of mental process-related potentials elicited prior to mental sweating response in humans. Neurosci Lett 1998; 247:25-8; PMID:9637401; http://dx.doi.org/10.1016/S0304-3940(98)00274-2
22. Henson RN, Friston KJ. Convolution models for fMRI. In: Friston K, Ashburner J, Kiebel S, Nichols T, Penny W, editors. Statistical Parametric Mapping: The analysis of functional brain images. London: Elsevier; 2006. p. 178-92.
23. Woolrich MW, Ripley BD, Brady M, Smith SM. Temporal autocorrelation in univariate linear modeling of FMRI data. Neuroimage 2001; 14:1370-86; PMID:11707093; http://dx.doi.org/10.1006/nimg.2001.0931
24. Birn RM, Smith MA, Jones TB, Bandettini PA. The respiration response function: the temporal dynamics of fMRI signal fluctuations related to changes in respiration. Neuroimage 2008; 40:644-54; PMID:18234517; http://dx.doi.org/10.1016/j.neuroimage.2007.11.059
25. Worsley KJ, Evans AC, Marrett S, Neelin P. A three-dimensional statistical analysis for CBF activation studies in human brain. J Cereb Blood Flow Metab 1992; 12:900-18; PMID:1400644; http://dx.doi.org/10.1038/jcbfm.1992.127